Self-Assembly of Heteroarms Core−Shell Polymeric Nanoparticles (HCPNs) and Templated Synthesis of Gold Nanoparticles within HCPNs and the Superparticles

Fei Cheng,[†] Kaka Zhang,[†] Daoyong Chen,*,[†] Lei Zhu,*,[‡] and Ming Jiang[†]

[†]*The Key Laboratory of Molecular Engineering of Polymers, Department of Macromolecular Science and Fudan University, Shanghai 200433, China, and [‡]Polymer Program, Institute of Materials Science and Department of Chemical, Materials and Biomolecular Engineering, University of Connecticut, Storrs, Connecticut 06269*

Received May 2, 2009; Revised Manuscript Received August 15, 2009

ABSTRACT: Here we report the self-assembly of heteroarm core−shell polymeric nanoparticles (HCPNs) into spherical superparticles and synthesis of gold nanoparticles within the HCPNs and the superparticles. HCPNs with polystyrene (PS)/poly(4-vinylpyridine) (P4VP) as the heteroarms and the cross-linked network poly(4VP-*co*-divinylbenzene) as the core were synthesized via a two-step anionic polymerization method. In the first step, living PS chains were prepared by initiating styrene using *n*-butyllithium in THF. In the second step, copolymerization of 4VP and DVB was initiated by the living PS chains. The HCPNs thus prepared have two features in the structure. (1) The HCPNs are large (the average hydrodynamic radius $\langle R_h \rangle$ of the HCPNs in DMF is 111 nm, whereas $\langle R_h \rangle$ of reported heteroarms star polymers are less than 10 nm) and flexible when they are dispersed in the solvents such as DMF and acidic water. (2) The PS arms are designed to be considerably longer than the P4VP arms. These two features led to interesting behaviors of the HCPNs in both the common solvent and the selective solvents for the heteroarms. In DMF, the common solvent, the HCPNs were swollen and with a $\langle R_h \rangle$ of 111 nm. In toluene, the selective solvent for PS, the longer PS arms shielded the short insoluble P4VP chains so that the HCPNs were individually dispersed with a $\langle R_h \rangle$ of 80 nm; the short P4VP arms collapsed, and the core shrank. In acidic water, which is a selective solvent for the shorter P4VP arms, the HCPNs self-assembled into large spherical superparticles with an average $\langle R_h \rangle$ of 187 nm. The above-mentioned two structural features are thought necessary for the regular self-assembly of such large and isotropic HCPNs. Furthermore, both HCPNs in toluene and the superparticles in acidic aqueous solution were used as templates to prepare gold nanoparticles (Au NPs). When HCPNs in toluene were used as the template, the Au NPs with a size of ca. 2−7 nm were scattered at the periphery of the cross-linked cores, forming raspberry-like morphology. When the superparticles were used as the template, the morphology of AuNP/superparticle composite nanoparticles depended on the solvent composition. In 0.1 M aqueous HCl solution, Au NPs were located at the periphery of the superparticles, forming gold shells with a thickness of ca. 50 nm. However, in 0.1 M HCl aqueous solution/DMF mixed solvent (9:1, v/v), the HAuCl₄ precursor could penetrate into the P4VP domains within the superparticles, forming dendron-like Au NP clusters within the template after the reduction.

Introduction

Recently, assembly using colloidal particles as building blocks has drawn great attention because "colloidal building blocks will be the "atoms" and "molecules" of tomorrow's materials."[1,2] For example, colloidal particles with homogeneous surfaces and a narrow size distribution have been used to construct colloidal crystals. By using liquid droplets as the template,[3−5] the "bricks and mortar" approach,[6,7] multidentate thioether ligands,[8−11] and biomolecules with complementary interactions,[12−14] "superparticles" with regular shapes and nano- to micrometer sizes were obtained from the assembly of colloidal particles. In addition, amphiphilic Janus particles have been proven to be ideal building blocks for construction of superparticles.[15−18] However, reports on superparticles derived from Janus particles are still limited due to the difficulty in preparing Janus particles that are capable of self-assembling into regular superparticles.

In the present study, heteroarms core−shell polymeric nanoparticles (HCPNs) with longer PS and shorter P4VP as the heteroarms and poly(4VP-*co*-DVB) cross-linked network as the core were prepared efficiently by a two-step anionic polymerization method. The behaviors of the HCPNs in the selective solvents for the heteroarms were studied. In toluene, a selective solvent for the longer PS arms, the HCPNs were individually dispersed with the shorter P4VP arms collapsed onto the cross-linked core. However, in acidic water, a selective solvent for the shorter P4VP arms, the HCPNs self-assembled into large spherical superparticles stabilized by the shorter quarternized P4VP arms. We believe that both the flexibility of the core and the difference between the lengths of P4VP and PS arms are responsible for the self-assembly of HCPNs. Furthermore, the HCPNs in toluene and the superparticles were used as templates to prepare gold NPs, leading to raspberry-, shell-, and dendron-like morphologies of the clusters of gold NPs, respectively. On the other hand, the morphologies of the clusters of gold NPs reflect the structures of the templates.

*Corresponding authors. E-mail: chendy@fudan.edu.cn (D.C.); lei.zhu@uconn.edu (L.Z.).

Experimental Section

Materials. Styrene, 4-vinylpyridine, and divinylbenzene were purchased from Aldrich and purified according to standard procedures for anionic polymerization. 1.6 M *n*-butyllithium in hexanes (Acros Organics), tetrachloroauric acid (HAuCl$_4$· 4H$_2$O, Aldrich), and sodium borohydride (NaBH$_4$, Aldrich) were used as received.

Preparation of PS/P4VP HCPNs. The HCPNs were prepared via a two-step sequential anionic polymerization. Living PS chains were prepared by anionic polymerization of styrene in THF at −78 °C, initiated by *n*-butyllithium. In the second step, a purified DVB/4VP mixture was added to the solution of living PS chains. The molar ratio of St/DVB/4VP in the reaction mixture was 10/1/10. The reaction was then kept at −78 °C for 10 h before terminated with degassed methanol. The final product was precipitated into *n*-hexanes for several times, and white powders were obtained. The relative molar contents of St, 4VP, and DVB in starting materials and products are shown in Table 2.

Synthesis of Au NPs within HCPN Templates in Toluene. Typically, 0.2 mL of HAuCl$_4$·4H$_2$O−DMF solution at a concentration of 45 mg/mL was added into 20 mL of HCPN toluene solution at a concentration of 2.0 mg/mL under strong magnetic stirring. The mixture solution was further stirred for 4 h, before 0.5 mL of NaBH$_4$ DMF solution at a concentration of 20 mg/mL was added dropwise. The reaction mixture was further stirred for 10 h.

Self-Assembly of PS/P4VP HCPNs in Acidic Water. In a typical procedure, 20 mg of HCPNs was dissolved in 6.0 mL of DMF under sonification for 30 min. 14 mL of aqueous HCl solution at pH = 1 was added dropwise (at a speed of 0.07 mL/min) into the DMF solution of HCPNs under magnetic stirring. The obtained solution was further dialyzed against 0.1 M HCl solution for 3 days. The final concentration of the polymer aqueous solution was roughly 1.0 mg/mL. Large spherical superparticles were thus obtained.

Synthesis of Au NPs within Large Spherical Superparticles. 4.5 mg of HAuCl$_4$·4H$_2$O was added into 10 mL of aqueous solution of the superparticles at ca. 1.0 mg/mL, followed by magnetic stirring in dark for 5 h. 2 mL of aqueous NaBH$_4$ solution at a concentration of 10 mg/mL was quickly added into the polymer solution with strong magnetic stirring. The color of the solution turned dark red immediately, indicating the formation of Au NPs. In this case, Au clusters formed in the superparticles are with a shell-like morphology. When we changed the 0.1 M HCl aqueous solution to 0.1 M HCl/DMF (v/v = 9/1) solution, dendron-like Au NP clusters were obtained within the superparticles.

Characterization Methods and Instruments. *Size-Exclusion Chromatography* (*SEC*). The number-average molecular weight (M_n) and polydispersity index (M_w/M_n) of the PS precursor polymer were determined using an Agilent 1100 equipped with a G1314A pump and a G1362A differential refractive index detector at 35 °C. THF was used as the eluent at a flow rate of 1.0 mL/min. PS standards were used for conventional calibration.

Elemental Analysis. Elemental analysis of HCPNs was performed on a Vario EL elemental analysis instrument (Elementar Co.).

^{1}H NMR Measurements. ^{1}H NMR measurements were performed on a Bruker DMX500 spectrometer in deuterated *N,N*-dimethylformamide (DMF-*d*$_7$).

Transmission Electron Microscopy (*TEM*). TEM observations were conducted on a Philips CM120 electron microscope at an acceleration voltage of 80 kV. Samples for TEM observations were prepared by casting a drop of solution onto a carbon-coated copper TEM grid and drying in ambient conditions. For observing the morphology of HCPNs in DMF, RuO$_4$ vapor was used for staining for 5 min. For observing the morphology of

Table 1. DLS Characterization Data of the HCPNs in DMF and Toluene and the Superparticles Formed in Acidic Water

solvent	$\langle R_h \rangle$ (nm)[a]	$\mu_2/\langle\Gamma\rangle^{2\,b}$
DMF	111	two peaks
toluene	80	two peaks
0.1 M aqueous HCl	187	0.08

[a] The average hydrodynamic radius. [b] The polydispersity index.

HCPNs in toluene, C$_4$H$_9$I (C$_4$H$_9$I/4VP = 1/1 mol/mol) was added into the toluene solution to stain the P4VP moieties. All polymer solutions for the TEM characterization were kept at a concentration of ca. 1.0 mg/mL.

Dynamic Light Scattering (*DLS*). A modified commercial light scattering spectrometer (ALV/SP-125) equipped with an ALV-5000 multi-τ digital time correlator and an ADLAS DPY425II solid-state laser (output power = 22 mW at λ = 632.8 nm) was used. All the DLS measurements were performed at 90° and 25°.

UV−vis Spectroscopy. The UV−vis spectroscopy was carried out on a Lambda 35 UV−vis absorption spectrometer (Perkin-Elmer).

Results and Discussion

Synthesis and Characterization of HCPNs. In this study, we simplified the three-step, arm-first anionic polymerization method for preparing heteroarm star polymers.[19−21] According to the three-step method, DVB should be added to the solution of living PS chains first and 4VP added after the exhaustion of DVB. Here, we used a two-step, arm-first approach to synthesize HCPNs; in the second step, a mixture of purified DVB and 4VP was added to the living PS chains (M_n = 93 100 g/mol and PDI = 1.12) in THF at −78 °C. The molar ratio of St/DVB/4VP in the reaction solution was 10/1/10. In such a way, grams of products can be obtained from a 100 mL solution. The molecular weight of the HCPNs was determined by static light scattering (SLS) to be 1.35 × 10^8 g/mol (S1 in the Supporting Information).

The as-prepared product was readily dissolved in organic solvents such as DMF and toluene. DLS measurements for the sample in DMF, which is a common solvent for PS and P4VP, showed that polymeric particles with an average hydrodynamic diameter ($\langle R_h \rangle$) as large as 111 nm were obtained (Table 1 and Figure 1). Obviously, such a large particle size implied that the core was formed by cross-linked network poly(4VP-*co*-DVB). In the cases of preparing star polymers using arm-first methods, where star polymers were with a core formed by pure multifunctional cross-linker, such as DVB, the radii of the star polymers were no more than 10 nm.[19−23] However, when the core was formed by copolymer of a cross-linker and a comonomer, the size increased remarkably.[24] The copolymerization of 4VP and DVB increased the size as well as the surface area of the core, leading to an increased number of arms in the final HCPN, because a larger number of arms were required to prevent further reactions between the core and other living species. In toluene, a selective solvent for PS, the $\langle R_h \rangle$ decreased to 80 nm (Table 1 and Figure 1), significantly smaller than that in DMF. This implied that the particles were individually dispersed in toluene and there were P4VP components in the particles whose shrinking led to the decrease of $\langle R_h \rangle$. A small peak at several nanometers is present in the two plots for the HCPNs, which should be associated with the dead macro-initiator. The individual dispersion of the particles in toluene was also proved by TEM observations (see below).

Characterizations by elemental analysis and ^{1}H NMR (Figure S2 in the Supporting Information) further confirmed that the core of the HCPNs was formed by
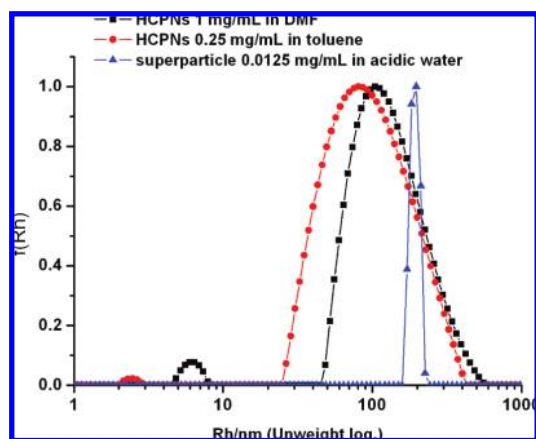
Figure 1. Hydrodynamic radius distributions (CONTIN plots) of the HCPNs in toluene (red curve) and in DMF (black curve) and the superparticles in acidic water at pH of 1.0 (blue curve).

Table 2. Relative Molar Contents of St, 4VP, and DVB in the Feed and HCPNs

	St	4VP	DVB
feed ratio	10.0	10.0	1.0
contents in HCPNs by EA[a]	10.0	9.1	1.0
contents in HCPNs by ^{1}H NMR[b]	10.0	6.5	

[a] The relative molar contents of St, 4VP, and DVB in polymeric particles were calculated according to the weight percents of carbon, nitrogen, and hydrogen obtained by elemental analysis (C, 86.12%; N, 6.48%; H, 7.38%). Elemental analysis could not determine the relative molar content of St (C_8H_8) to DVB ($C_{10}H_{10}$) due to the same number ratio of C to H atom in both molecules. Because the reactivity of DVB in an anionic polymerization is high and the reaction time is as long as 10 h, we assumed that all the DVB were polymerized. [b] The ^{1}H NMR method could not detect the signal of DVB because of its reduced mobility due to cross-linking.[25]

poly(4VP-*co*-DVB) network and there are P4VP arms (shorter than the PS arms) in the HCPNs. As mentioned before, the molar feed ratio of St/DVB/4VP in the reaction mixture was 10/1/10. Elemental analysis results in Table 2 indicated that the St/DVB/4VP molar ratio in the HCPNs was 10/1/9.1 with 4VP content slightly lower than that in the feed ratio. ^{1}H NMR results (measured in DMF-d_7) in Table 2 also clearly showed the presence of P4VP in the HCPNs. However, the 4VP/St molar ratio is 6.5/10 (Table 2), much lower than the ratio 9.1/10 determined by elemental analysis. We conclude that some 4VP units were located in the core because only these 4VP units that were located in the core (formed by poly(4VP-*co*-DVB) cross-linked network) were with mobility too low to be detected by ^{1}H NMR.[25] The ratio of these 4VP units undetectable by ^{1}H NMR is 0.26 (i.e., 0.91−0.65), relative to styrene units. However, we believe that these 4VP units undetectable by ^{1}H NMR are only a part of the 4VP units located in the core. In other words, not all the 4VP units in the core are undetectable by ^{1}H NMR. Because the core was swollen in DMF, as indicated by the large difference between the average hydrodynamic diameter ($2\langle R_h\rangle$) of the HCPNs in DMF and the size observed by TEM (see below), some long P4VP loops between cross-linking points should have enough mobility to be detected by ^{1}H NMR. Therefore, the ratio of 4VP units in the core is larger than 0.26 (relative to styrene units), or the ratio of 4VP in the arms is less than 0.65 (0.91−0.26). In the heteroarms of the HCPNs, the PS arms were longer than the P4VP arms with a length ratio >1/0.65. Nevertheless, there are still P4VP arms (i.e., not all 4VP units were located
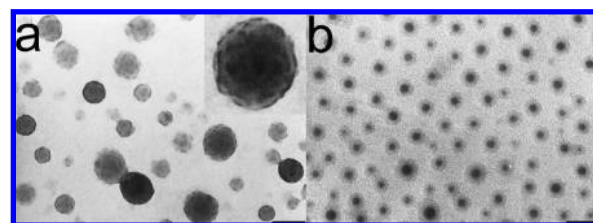

Figure 2. TEM images of polymeric nanoparticles: (a) cast from a common solvent, DMF, and stained by RuO_4 and (b) cast from toluene and stained with C_4H_9I. The scale bars are 100 nm.

in the core). This conclusion is based on TEM observations of the HCPNs cast from DMF (explained below) and the consideration on the kinetics of DVB and 4VP anionic copolymerization. Because the molar ratio of 4VP/DVB in the feed was 10/1 and DVB is more reactive than 4VP in an anionic polymerization,[21] there should be 4VP monomer remained after the exhaustion of DVB to form graft arms.

To further characterize the structure of the HCPNs in DMF, we observed them using TEM. Figure 2a shows RuO_4-stained HCPNs cast from DMF, a common solvent for the PS/P4VP heteroarms. It was reported that P4VP is more susceptible to RuO_4 staining than PS.[26] In the TEM image, P4VP formed isolated domains with a relatively high contrast within the nanoparticles (see the inset in Figure 2a). This is consistent with the fact that P4VP is the minor component in the nanoparticles. Moreover, many P4VP domains appeared to locate near the edge of the nanoparticles rather than in the center. This result suggested that the P4VP microdomains were formed by grafted P4VP arms mixed with PS arms. The diameter of the nanoparticles in the TEM image ranged from 35 to 105 nm, much smaller than that observed by DLS. This indicates the swollen structure of the HCPNs in DMF. The large decrease in size must result from the chain collapse and shrinking of the nanoparticles during solvent evaporation on copper grids. Considering the fact that the core of the HCPNs was formed by poly(4VP-*co*-DVB) network that was highly swollen in DMF, the HCPNs are similar to microgels to a certain extent.

Different from the morphology in Figure 2a, a typical micrograph of n-C_4H_9I stained HCPNs cast from toluene is shown in Figure 2b. In the selective solvent for PS arms, the longer PS chains shielded the shorter insoluble P4VP chains and prevented further nanoparticle aggregation. P4VP chains collapsed onto the core of the HCPNs, leading to core−shell morphology with dark P4VP in the central area of the particles (Figure 2b). It should be mentioned here that there is no PS-*b*-P4VP block copolymer in the HCPNs, which was thought to be possibly produced during preparing the HCPNs and could self-assemble in toluene to form aggregates similar to the nanoparticles in Figure 2b. We characterized the HCPNs by size exclusion chromatography using DMF as the eluent but did not detect any signals possibly related to the block copolymer. This is understandable that, due to the high reactivity of DVB in the anionic polymerization, it is impossible that, in the polymerization, there are considerable amount of macroinitiator that only initiated 4VP molecules to form PS-*b*-P4VP block copolymer without initiating DVB.

Now, the formation mechanism for the HCPNs is clear. During the second step polymerization, PS macroinitiator initiated the copolymerization of DVB and 4VP, forming the core. After the exhaustion of DVB, the carbanions in the core started to initiate the polymerization of remaining 4VP monomers, forming the shorter P4VP arms.
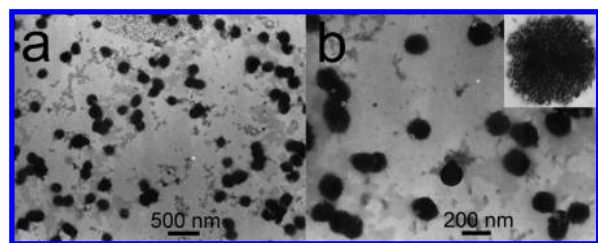
Figure 3. TEM images of large spherical superparticles self-assembled from the HCPNs in 0.1 M HCl solution. Both (a) and (b) are the superparticles but with different magnifications.

Figure 4. Schematic representation of the large regular spherical super-particle formation.

Self-Assembly of PS/P4VP HCPNs in Acidic Aqueous Solution. In acidic water, a selective solvent for P4VP (P4VP is soluble in acid water when the pH value is below 4.8), the longer insoluble PS arms could not be sufficiently shielded by the shorter soluble P4VP arms. Interparticle aggregation may occur. Experimentally, the HCPNs were first dissolved in DMF, and 0.1 M aqueous HCl solution was then added into the DMF dispersion until the volume ratio of water/DMF was 7/3. The scattering light intensity increased dramatically upon the addition of acidic water, indicative of the formation of large aggregates. The solution was then dialyzed against 0.1 M HCl solution for 3 days to remove DMF. In the resultant solution, the concentration of the HCPNs was about 1.0 mg/mL. The prepared polymer aqueous solution remained stable for months without any precipitation. DLS measurements demonstrated the formation of large particles with a $\langle R_h \rangle$ of 187 nm. The polydispersity index $(\mu_2/\langle\Gamma\rangle^2)$ was as low as 0.08, demonstrating the narrow size distribution of the particles formed in the acidic water (Figure 1 and Table 1). Obviously, these particles must be formed by the primary HCPNs and can be termed as superparticles (S1 in the Supporting Information).

The superparticles were observed by TEM without any staining (Figure 3). The large spherical superparticles had an average diameter of about 190 nm in the TEM images. Compared with the DLS result, these superparticles shrank upon solvent evaporation during TEM sample preparation. In a magnified TEM image of a superparticle as the inset in Figure 3b, it shows a "porous" morphology. In the TEM image of the superparticles without staining, the contrast of a domain is determined by its thickness and density. The pores with a low contrast should originate from the P4VP domains that are protonated and originally swollen in the acidic water. After the evaporation of water on copper grid, the swollen protonated P4VP domains shrank and left the pores (note that the protonated P4VP domains within the super-particles should be surrounded by the rigid PS domains). Considering the large regular spherical superparticles, we think that the HCPNs that are originally spherical and with a large core must have deformed a lot to build the super-particles. As mentioned before, there are a large amount of 4VP units in the core. The solubility of the 4VP units in the core in the acidic water resulted in the swelling of the core. The swelling made the core flexible and the deformation possible. Besides, there seems a similarity between the superparticles and the supermicelles/the compound micelles reported by Eisenberg et al.[27,28] Both the superparticles and the super-micelles/the compound micelles were formed by primary core−shell particles. However, since each of the HCPNs within the superparticles is not dissociable, this should result in dissimilarities in the structure and properties between the superparticles and the supermicelles/the compound micelles.

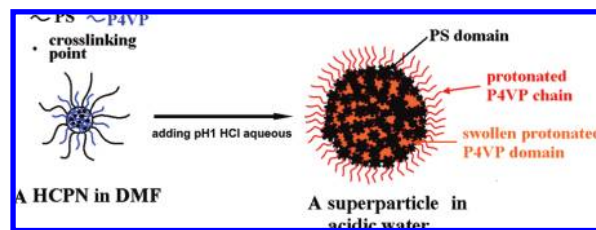Tsitsilianis et al.[23] reported the association behavior of PS/P2VP heteroarm star copolymers in acidic water. Different from the HCPNs, the star copolymer was with a small size (the average molecular weight of the star copolymer is only ca. 5×10^5) and a rigid core. Besides, in contrast to the HCPNs, in the star copolymer, the P2VP arms are longer than the PS arms. These made the association between the star copolymer in acidic water difficult, as indicated by the large critical micellization concentration (cmc) (10 mg/mL). The high cmc implies that the supermicelles in acid water are unstable and coexist with a large amount of the unimolecular star copolymer. This may limit potential applications based on the supermicelles. More recently, worm-like super-particles resulted from the self-assembly of heteroarm star polymers, and heteroarm star hybrid particles were re-ported.[29−32] In all these heteroarm star particles, the ratio of the arm length to the core diameter was very large. In selective solvents, the relatively small core size allowed the solvophilic arms fully phase separate from the solvophobic arms to form amphiphilic Janus-like primary particles, which were capable of self-assembling into superparticles. In this study, Janus-like primary particles could not form by phase separation between the PS arms and the P4VP arms because of the relatively large core size and short P4VP arms (they are not long enough to circumvent the core). Instead, many quarternized P4VP microdomains were encapsulated within the superparticles, together with collapsed PS arms. Intriguingly, as the aggregates grew bigger, the soluble protonated P4VP arms at the periphery were able to prevent further growth and finally stabilize the superparticles in acidic aqueous solution. The uniform size of the supermi-celles suggests a balance between particle aggregation and steric repulsion from quarternized P4VP arms between two superparticles. Therefore, these superparticles are promising templates for controlled synthesis of hybrid nanoparticles with various architectures.

Synthesis of Au NPs within PS/P4VP HCPN Templates in Toluene. Block copolymer micelles in selective solvents have been widely used as templates to synthesize inorganic nano-particles. The prepared inorganic nanoparticles are stabi-lized by being attached to the polymeric micelles. However, when the polymeric micelles dissociate due to changes in solvent and/or temperature, the inorganic nanoparticles may easily aggregate and precipitate out from solutions. Compared to block copolymer micelles, unimolecular mi-celles have much better stability against environmental changes.[33,34] Therefore, when unimolecular micelles are used as templates, the loss of the stability of the inorganic nanoparticles in solution due to the dissociation of polymeric micelles can be avoided. Actually, each of the HCPNs can be considered as a huge molecule with a cross-linked core-soluble shell structure. The unique distribution of P4VP component in the HCPNs, which are the versatile interacting component for binding inorganic species, makes the HCPNs promising as special templates for the synthesis of inorga-nic nanoparticle (e.g., gold or silver) with an interesting architecture.
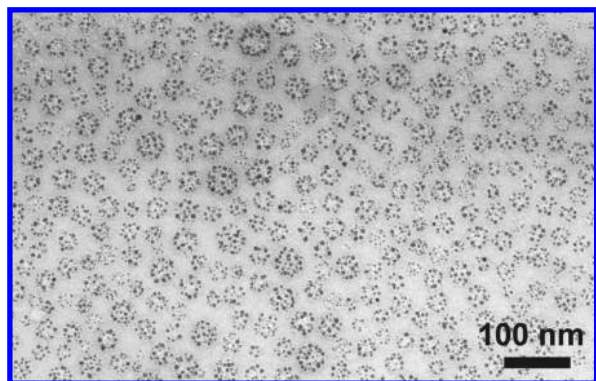
Figure 5. TEM image of Au NP/HCPN hybrids prepared by forming Au NPs within HCPNs in toluene.

To prepare Au NP/HCPN hybrid nanoparticles in toluene, a small amount of $HAuCl_4 \cdot 4H_2O$ solution in DMF was mixed and fully interacted with HCPNs in toluene, followed by reducing $HAuCl_4$ precursor with $NaBH_4$. The resultant hybrid nanoparticles were well-stabilized in toluene, and no precipitate was observed during storage for several months. The hybrid nanoparticles cast from toluene were examined by TEM, as shown in Figure 5. The small dark spheres with a size in the range of 2−7 nm are Au NPs, and they gather around the cross-linked cores of the HCPNs. From the TEM image in Figure 5, we can see clusters (each of the clusters is formed by the small Au NPs within one HCPN) with a size comparable to that of the core of the HCPNs (Figure 2b). From this result, we infer that $HAuCl_4$ precursors selectively bound to the collapsed P4VP arms around the cores of HCPNs in toluene. Note that the cross-linked cores (including cross-linked P4VP and DVB) in toluene should be compact, and no $HAuCl_4$ precursor could access their inner parts. After chemical reduction using $NaBH_4$, raspberry-type morphology is thus observed in the TEM micrograph in Figure 5. These hybrid nanoparticles were stable in toluene due to the steric protection from the soluble long PS arms and did not disintegrate even after dilution with 10 times the volume of a common solvent, DMF, because of the chemical cross-linking of the cores. Additionally, for most Au NPs/polymeric micelle composite NPs, the Au NPs were usually encapsulated in the core of the micelles.[35,36] When used as catalyst, these Au NPs may have a decreased activity because their contact with reactants could be limited since they are encapsulated in the core. For the Au NP/HCPN hybrids, the majority of AuNPs are located outside of the cross-linked core. They are more exposed to reaction media and reactants and thus more reactive than the Au NPs encapsulated in the core.[37,38]

Synthesis of AuNPs within Superparticle Templates. The Au NP/superparticle hybrid nanoparticles were prepared by mixing $HAuCl_4$ with the superparticles in acidic water, followed by reducing $HAuCl_4$ with $NaBH_4$. The as-prepared Au NP/superparticle hybrid nanoparticles exhibited a red color in 0.1 M acidic solution. The aqueous suspension is very stable, since no obvious changes had been seen during storage for months. These Au NP/superparticle hybrid particles were characterized by UV−vis spectroscopy, which showed a maximum absorption at 530 nm (Figure 6b), confirming the formation of Au PNs. In the TEM image in Figure 6a, most Au NPs locate in the peripheral of the superparticles with a shell-like morphology for the hybrid nanoparticles. The Au shell thickness was roughly 50 nm. Although prolonged time and excessive $HAuCl_4$ were used to prepare Au NPs using these superparticles in the acidic
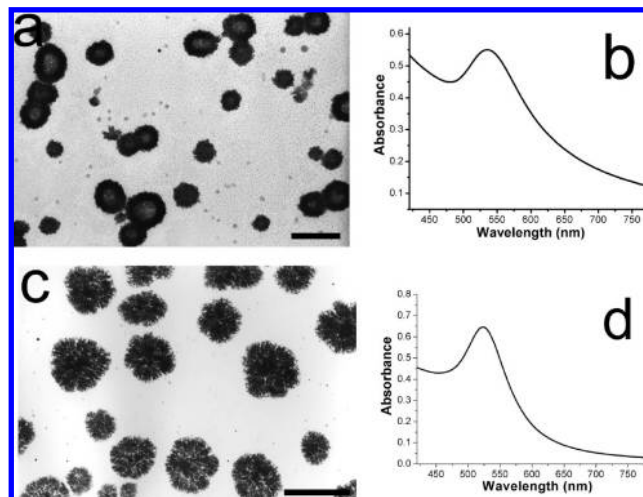

Figure 6. TEM images of Au NPs/superparticle hybrid nanoparticles in pH 1 HCl (a) and in mixture of pH 1 HCl/DMF (9/1, v/v) (c). UV−vis spectra of Au NP/superparticle composites in pH 1 HCl (b) and in mixture of pH 1 HCl/DMF (9/1, v/v) (d). The scale bars represent 200 nm.

water, the same shell-like morphology was observed as in Figure 6a. This indicates that the protonated P4VP domains encapsulated in the superparticles may be so isolated by hydrophobic PS domains and/or the cores of the superparticles are so dense that $HAuCl_4$ cannot access the inside.

To allow $HAuCl_4$ to penetrate into the inside of the superparticles, we used mixed water/DMF solvent (9/1, v/v) to prepare Au NP/superparticle hybrid nanoparticles, while keeping other conditions unchanged. A dendritic morphology was observed in the TEM image in Figure 6c. Apparently, DMF in the mixed solvent swelled the hydrophobic PS domains, and the cores of superparticles became loose. This allowed the diffusion of $HAuCl_4$ into the encapsulated $P4VPH^+Cl^-$ domains. Therefore, the resultant hybrid nanoparticles exhibit dendron-like morphology. The maximum absorption in the UV−vis spectrum is at 523 nm (Figure 6d), again suggesting the formation of Au NPs. Note that the dendron-like morphology has not been reported for AuNPs clusters before.

Conclusions

In conclusion, a two-step anionic polymerization method was used to synthesize PS/P4VP HCPNs with long PS arms and short P4VP arms grafted to DVB cross-linked cores. These HCPNs exhibited different behaviors in both common (DMF) and selective (toluene and acidic water) solvents, respectively. In DMF, the individual HCPN had a swollen core with a relatively large $\langle R_h \rangle$. In toluene, the HCPNs exhibited a core−shell morphology with P4VP arms collapsed onto the core and PS stretching out in the corona. In 0.1 M acidic water, however, short and quarternized P4VP arms became soluble, and the HCPNs self-assembled into large regular spherical superparticles through the hydrophobic interaction of long PS arms. Both single HCPNs in toluene and the superparticles in acidic aqueous solution were used as templates to prepare Au NPs. Raspberry-, shell-, and dendron-like morphologies for the hybrids were observed. Especially, different morphologies, (shell- vs dendron-like) of the Au NP/superparticle hybrids could be easily controlled by the solvent composition. For example, in 0.1 M aqueous HCl solution, the composite particles were shell-like, while in 0.1 M aqueous HCl/DMF (9/1 v/v) mixed solvent, dendron-like Au NP/LRSA composite particles were obtained.

Supporting Information Available: Static light scattering results of the HCPNs in toluene and the superparticles in acidic water at pH of 1.0; ^{1}H NMR spectrum of the HCPNs in DMF-d_7. This material is available free of charge via the Internet at http://pubs.acs.org.

References and Notes

(1) Glotzer, S. C. *Science* **2004**, *306*, 419–420.
(2) Glotzer, S. C.; Solomon, M. J. *Nat. Mater.* **2007**, *6*, 557–562.
(3) Manoharan, V. N.; Elsesser, M. T.; Pine, D. J. *Science* **2003**, *301*, 483–487.
(4) Cho, Y. S.; Yi, G. R.; Lim, J. M.; Kim, S. H.; Manoharan, V. N.; Pine, D. J.; Yang, S. M. *J. Am. Chem. Soc.* **2005**, *127*, 15968–15975.
(5) Maenosono, S.; Dushkin, C. D.; Saita, S.; Yamaguchi, Y. *Langmuir* **1999**, *15*, 957–965.
(6) Boal, A. K.; Ilhan, F.; DeRouchey, J. E.; Thurn-Albrecht, T.; Russell, T. P.; Rotello, V. M. *Nature* **2000**, *404*, 746–748.
(7) Shenhar, R.; Rotello, V. M. *Acc. Chem. Res.* **2003**, *36*, 549–561.
(8) Maye, M. M.; Chun, S. C.; Han, L.; Rabinovich, D.; Zhong, C. J. *J. Am. Chem. Soc.* **2002**, *124*, 4958–4959.
(9) Maye, M. M.; Luo, J.; Lim, I. I. S.; Han, L.; Kariuki, N. N.; Rabinovich, D.; Liu, T. B.; Zhong, C. J. *J. Am. Chem. Soc.* **2003**, *125*, 9906–9907.
(10) Maye, M. M.; Lim, I. I. S.; Luo, J.; Rab, Z.; Rabinovich, D.; Liu, T. B.; Zhong, C. J. *J. Am. Chem. Soc.* **2005**, *127*, 1519–1529.
(11) Lim, I. I. S.; Pan, Y.; Mott, D.; Ouyang, J.; Njoki, P. N.; Luo, J.; Zhou, S. Q.; Zhong, C. J. *Langmuir* **2007**, *23*, 10715–10724.
(12) Mirkin, C. A.; Letsinger, R. L.; Mucic, R. C.; Storhoff, J. J. *Nature* **1996**, *382*, 607–609.
(13) Storhoff, J. J.; Lazarides, A. A.; Mucic, R. C.; Mirkin, C. A.; Letsinger, R. L.; Schatz, G. C. *J. Am. Chem. Soc.* **2000**, *122*, 4640–4650.
(14) Wang, G. L.; Murray, R. W. *Nano Lett.* **2004**, *4*, 95–101.
(15) Erhardt, R.; Boker, A.; Zettl, H.; Kaya, H.; Pyckhout-Hintzen, W.; Krausch, G.; Abetz, V.; Mueller, A. H. E. *Macromolecules* **2001**, *34*, 1069–1075.
(16) Erhardt, R.; Zhang, M. F.; Boker, A.; Zettl, H.; Abetz, C.; Frederik, P.; Krausch, G.; Abetz, V.; Muller, A. H. E. *J. Am. Chem. Soc.* **2003**, *125*, 3260–3267.
(17) Nie, L.; Liu, S. Y.; Shen, W. M.; Chen, D. Y.; Jiang, M. *Angew. Chem., Int. Ed.* **2007**, *46*, 6321–6324.
(18) Cheng, L.; Zhang, G. Z.; Zhu, L.; Chen, D. Y.; Jiang, M. *Angew. Chem., Int. Ed.* **2008**, *47*, 10171–10174.
(19) Tsitsilianis, C.; Voulgaris, D. *Macromol. Chem. Phys.* **1997**, *198*, 997–1007.
(20) Hadjichristidis, N.; Pitsikalis, M.; Pispas, S.; Iatrou, H. *Chem. Rev.* **2001**, *101*, 3747–3792.
(21) Hadjichristidis, N.; Pispas, S.; Iatrou, H.; Pitsikalis, M. *Curr. Org. Chem.* **2002**, *6*, 155–176.
(22) Voulgaris, D.; Tsitsilianis, C.; Esselink, F. J.; Hadziioannou, G. *Polymer* **1998**, *39*, 6429–6439.
(23) Tsitsilianis, C.; Voulgaris, D.; Stepanek, M.; Podhajecka, K.; Prochazka, K.; Tuzar, Z.; Brown, W. *Langmuir* **2000**, *16*, 6868–6876.
(24) Gao, H. F.; Matyjaszewski, K. *Macromolecules* **2006**, *39*, 3154–3160.
(25) Chen, D.; Peng, H.; Jiang, M. *Macromolecules* **2003**, *36*, 2576–2578.
(26) Saito, R.; Fujita, A.; Ichimura, A.; Ishizu, K. *J. Polym. Sci., Part A: Polym. Chem.* **2000**, *38*, 2091–2097.
(27) Zhang, L. F.; Eisenberg, A. *Science* **1995**, *268*, 1728–1731.
(28) Duxin, N.; Liu, F. T.; Vali, H.; Eisenberg, A. *J. Am. Chem. Soc.* **2005**, *127*, 10063–10069.
(29) Teng, J.; Zubarev, E. R. *J. Am. Chem. Soc.* **2003**, *125*, 11840–11841.
(30) Xu, J.; Zubarev, E. R. *Angew. Chem., Int. Ed.* **2004**, *43*, 5491–5496.
(31) Zubarev, E. R.; Xu, J.; Sayyad, A.; Gibson, J. D. *J. Am. Chem. Soc.* **2006**, *128*, 4958–4959.
(32) Zubarev, E. R.; Xu, J.; Sayyad, A.; Gibson, J. D. *J. Am. Chem. Soc.* **2006**, *128*, 15098–15099.
(33) Djalali, R.; Li, S. Y.; Schmidt, M. *Macromolecules* **2002**, *35*, 4282–4288.
(34) Zhang, M. F.; Drechsler, M.; Muller, A. H. E. *Chem. Mater.* **2004**, *16*, 537–543.
(35) Forster, S.; Antonietti, M. *Adv. Mater.* **1998**, *10*, 195–+.
(36) Jaramillo, T. F.; Baeck, S. H.; Cuenya, B. R.; McFarland, E. W. *J. Am. Chem. Soc.* **2003**, *125*, 7148–7149.
(37) Lu, Y.; Mei, Y.; Drechsler, M.; Ballauff, M. *Angew. Chem., Int. Ed.* **2006**, *45*, 813–816.
(38) Wen, F.; Zhang, W. Q.; Wei, G. W.; Wang, Y.; Zhang, J. Z.; Zhang, M. C.; Shi, L. Q. *Chem. Mater.* **2008**, *20*, 2144–2150.